Ab Initio Study of Defect Sites at the Inner Surfaces of Mesoporous Silicas

E. Fois,[†] A. Gamba,[†] G. Tabacchi,*[,†] S. Coluccia,[‡] and G. Martra[‡]

Dipartimento di Scienze CFM, Universita' dell'Insubria, and INSTM, UdR Como, Via Lucini 3, I-22100 Como, Italy, and Dipartimento di Chimica IFM, Universita' di Torino, and INSTM, UdR Universita' Torino, via Giuria 7 I-10125 Torino, Italy

Received: July 25, 2003

Ab initio molecular dynamics simulations on 1-nm thick slabs of amorphous silica have been carried out in order to mimic the local properties of mesoporous materials framework. A number of defects have been considered, both with closed and open shell electronic structure, and their spectroscopic properties analyzed and compared with experiments. The "strained siloxane bridge" defect has been studied in detail and its possible radical nature highlighted.

Introduction

Mesoporous ordered molecular sieves[1] are extremely promising materials characterized by high specific surface area (∼1000 m^2/g),[1−3] significantly larger with respect to more conventional highly dispersed oxide materials, and pores with diameters ranging from 15 to 150 Å,[1,2] thus larger than those normally found in crystalline microporous materials such as zeolites (<15 Å).[4] Several types of such mesoporous materials are known (i.e., M41S, FSM, and SBA),[3] and among them, the MCM-41, of the M41S family, received the greatest attention. The structure of MCM-41 may be described as a regular lattice of parallel (non crossing) empty channels surrounded by a matrix (framework) of amorphous silica (a-SiO_2). As the walls between channels have thicknesses of the order of 1 nm, their properties should closely resemble those of nanosized silica layers, thus opening the way to novel applications in advanced nanoscale technology.[5,6] Like other a-SiO_2 materials, MCMs absorb photons in the UV range and then relax by emitting visible light.[5−9] These photoluminescence (PL) properties have been attributed to point defects in the a-SiO_2 matrix and may depend on the preparation conditions of the materials.[5−15] Some examples among the many postulated defect structures are the nonbridging oxygen hole centers (NBOHC) ≡Si−O$^\bullet$ (where the three lines indicate bonds with three oxygen atoms), the peroxy-radicals ≡Si−O−O$^\bullet$, the surface E′ centers ≡Si$^\bullet$, and the oxygen vacancies ≡Si−Si≡.[10−15] As such point defects are embedded in an amorphous matrix, the relationship between optical properties and microscopic structure is not thoroughly understood yet. In addition, as evidenced by many PL studies, the properties of a defect are strongly influenced by its local environment, in particular by the presence of other defects in the neighborhood.[5−15] In vibrational spectroscopies, the so-called "silica-window" is a semitransparent region (800÷1000 cm^{-1}) laying between the Si−O−Si symmetric and asymmetric stretching modes in nonstrained and unperturbed conditions for the SiO_4 tetrahedra network.[16,17] All perturbations to this standard situation lead in particular to a weakening of the Si−O bonds and therefore to a red-shift of the Si−O−Si asymmetric stretching modes. In the limiting case where the Si−O−Si chain is broken, a ≡Si−O single oscillator will be present,[16] which may be saturated with H (giving rise to a silanol) or not (e.g., a ≡Si−O$^\bullet$ radical). The characteristic frequencies of such a single oscillator will however be found inside the silica window; for instance, ≡Si−OH stretching modes give rise to bands in the region 960−990 cm^{-1} of the IR spectra of both amorphous and crystalline silicates.[10,18−20] Chemical reactivity is a probe for studying the point defect structure as well, and the integration of vibrational and electronic spectroscopy with reactivity analysis is a constructive approach to such problems. Very reactive sites are formed on the surface of both MCMs and bulk a-SiO_2 when dehydrated at temperatures higher than ∼600 °C.[21−29] These sites show a very high Lewis acidity toward pyridine and trimethylamine,[21] allow the dissociative chemisorption of water, ammonia, and methanol,[22−25,28] and are also involved in some photocatalytic reactions.[29] Their characteristic IR features are two weak bands around 890 and 910 cm^{-1} in the silica-window, which disappear upon water or ammonia chemisorption.[21−29] Moreover, a band at 890 cm^{-1} has also been observed for crystalline microporous silicates outgassed at high temperatures.[16] The structure of such a defect, known as "strained siloxane bridge" (SSB),[21] is not firmly established yet. One of the structural models proposed is the 2M-defect or 2M-ring, which consists of an extremely strained $(Si−O)_n$ ring ($n = 2$) formed by two edge sharing SiO_4 tetrahedra (Figure 1), whose internal Si−O−Si and O−Si−O angles are much distorted with respect to their ideal tetrahedral values. Both experimental and theoretical data suggested that the presence of edge-sharing 2M-defects may be compatible with the observed properties of the surface.[24,25,27,30] On the other hand, a recent IR/VUV/ESR study on a series of silica materials (including MCM-41) strongly supports the idea that the SSBs should be radical species, as the presence of the two IR defect bands is accompanied by ESR signals.[29] It should be stressed, however, that in many studies the materials resulted ESR-silent.[21−25] For the sake of completeness, we recall that some authors attributed to the SSB also a band at ∼930−940 cm^{-1}.[21−23,27]

It is clear from this picture that further investigation is needed in order to single out, among the many postulated defect centers (e.g., three- and four-membered rings[31] (Figure 1), 2M rings,

* To whom correspondence should be addressed. E-mail: gloria@fis.unico.it. Fax: ++39 31 326230.
[†] Universita' dell'Insubria.
[‡] Universita' di Torino.

10.1021/jp036182b CCC: $25.00
Published on Web 09/06/2003

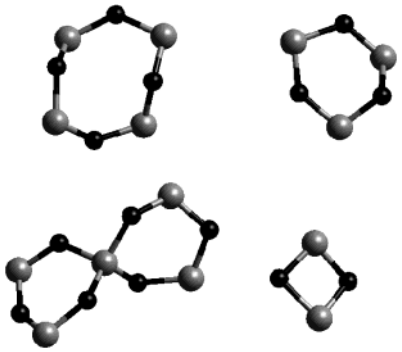

Figure 1. Schematic structural models of the $(Si-O)_n$ strained rings defect centers. From top-left to bottom-left, clockwise: 4-ring, $(Si-O)_4$; 3-ring, $(Si-O)_3$; 2M-ring, $(Si-O)_2$; two 3-rings sharing one vertex (i.e. spiro-5^4), Si_5O_6. Grey spheres: Si; black spheres: O. Only the O atoms forming the cycles have been represented.

and paramagnetic defects), the most likely structural models for the SSBs. Because both strained and, in the limiting case, broken Si−O−Si bridges can show bands inside the silica window, many different defect centers could in principle be responsible of the two IR "defect-bands". Thus, a relatively wide range of possible structural defects has been modeled in this work, even if their concentration may be out of the experimentally detectable range.

Here we report results of ab initio molecular dynamics simulations[32] of nanothick silica slabs modeling the thinnest part of the walls separating the pores in MCM materials. The simulated layers were designed in such a way to reproduce the experimentally determined wall thickness (about 10 Å) and surface silanol density (~2 OH/nm^2)[33] in a slab geometry with periodic boundary conditions. The slab was built in a three-dimensional periodic MD cell of $8.5 \times 8.5 \times 17$ Å^3. Each model layer presents two surfaces parallel to the *xy* plane and exhibits different kinds of structural defects. As the layer thickness is about 10 Å, in the model, a vacuum region of about 7 Å is present in order to minimize intersurfaces interactions. Our purpose is to compare the properties of the simulated layers with the available experimental data and try to correlate the presence of a given property to the microscopic structure of the layer.

The models proposed here do not reproduce the curvature of the MCM-41 inner walls. To fully take into account the effective curvature, much larger simulation systems would have been required. However, optical fibers and silica nanoparticles are characterized by surfaces with a curvature of opposite sign with respect to the inner walls of MCM-41, though show similar spectroscopic properties attributed to the same types of defects.[11,14,15] This may be assumed as a suggestion that the effect of surface curvature should not be relevant, at least to a first approximation.

Calculations

Ab initio MD simulations[34] were performed on three silica slabs, characterized by chemical formula $m(SiO_2) + n(H_2O)$ (with $m = 10$ and 11 and $n = 1$ and 2). In all simulations, the electronic structure was calculated by DFT with gradient corrected approximations for the exchange and correlation energies.[35−36] We used a plane waves cutoff of 60 Ry for the wave functions. Only valence electrons were explicitly described, whereas the core electrons were treated via norm-conserving pseudopotentials[37,38] (d-nonlocality for Si and O, and a local pseudopotential for H). We adopted an electronic fictitious mass of 500 au, a MD time step of 0.121 fs, and a target simulation temperature of 298 K (NVT ensemble).[39]

Because of the amorphous nature of the simulated samples, no experimental atomic positions were available as input for the MD runs. The initial coordinates were obtained by cutting a slice of ~1 nm thickness from a silica glass configuration. The unsaturated Si/O atoms were then gradually removed by a simulated annealing procedure and by adding water molecules. After equilibration, data were collected from simulation runs of ~10 ps elapsed time each.

Our simulated systems are characterized by a high density of topological defects such as strained $(Si-O)_n$ rings (shown in Figure 1), but no chemical disorder (i.e., wrong Si−Si or O−O bonds) is present. All of the model layers have proved to be stable along MD runs.

The simulated layers are schematically represented in Figure 2. In the first one, S0 (with $m = 10$, $n = 1$), both surfaces exhibit an isolated silanol. The two silanols are attached to two adjacent 4-rings, and in addition, one of the silanols is also bonded to a 3-cycle. Also the second model slab, S1 ($m = 11$, $n = 2$), shows strained rings. Two geminal silanols are present on a surface, whereas the other surface shows two vicinal silanols. S1 contains also a very strained arrangement of tetrahedra composed by two 3-rings sharing a vertex. The third simulated layer, S2 (m=11, n=1), was obtained from S1 by removing a water molecule from the two vicinal silanols, thus forming the 2M defect. To explore also the hypothesis that the SSB could have a radical nature, we have performed two additional simulations starting from randomly chosen configurations from system S2 and adopting the restricted-open shell Kohn−Sham formalism (ROKS).[40]

Results and Discussion

As already pointed out, our nanothick layers exhibit 3- and 4-rings, and in S2, also the 2M defect is present. As the concentration of such defects is relatively high, we expect that the structural properties (i.e., bond distances and angles) in the simulated layers should be different from those shown by crystalline SiO_2 or by bulk a-SiO_2. The average Si−O−Si angles calculated for S0 (134°), S1 (140°), and S2 (133°) are lower than the values typical of undistorted tetrahedral networks (e.g., 144° for α-quartz),[41] indicating that the slabs are characterized by a high degree of strain. Moreover, the average Si−O distances (1.672, 1.667, and 1.682 Å for S0, S1, and S2 respectively) are about 3% larger than the values calculated for porous crystalline aluminosilicates (zeolites) using the same computational techniques.[42]

The calculated vertical excitation spectra of the three slabs, shown in Figure 3, were obtained using 60 excited states and averaging over 20 uncorrelated configurations for each system. The well-known DFT systematic underestimation of calculated electronic energy gaps (and transition energies) prevents quantitative agreement with experiments. Nevertheless, comparison of simulated excitation spectra provide useful insight on how structural changes may affect the electronic properties of the material. Although the S0 and S1 spectra are very similar, the edge of absorption in the S2 spectrum significantly shifts toward lower energies. This effect should be unambiguously attributed to the presence of the 2M rings. Other possible "candidates" in the S2 slab (e.g., 3- and 4-rings) are excluded because they are present on all the studied layers. Therefore, these data indicate for the first time that the formation of 2M-rings on a nanothick silica surface perturbs its electronic spectra. Many experimental studies report that high-temperature pretreatment of MCM materials leads to the appearance of new bands in the UV/vis region in both the excitation and emission

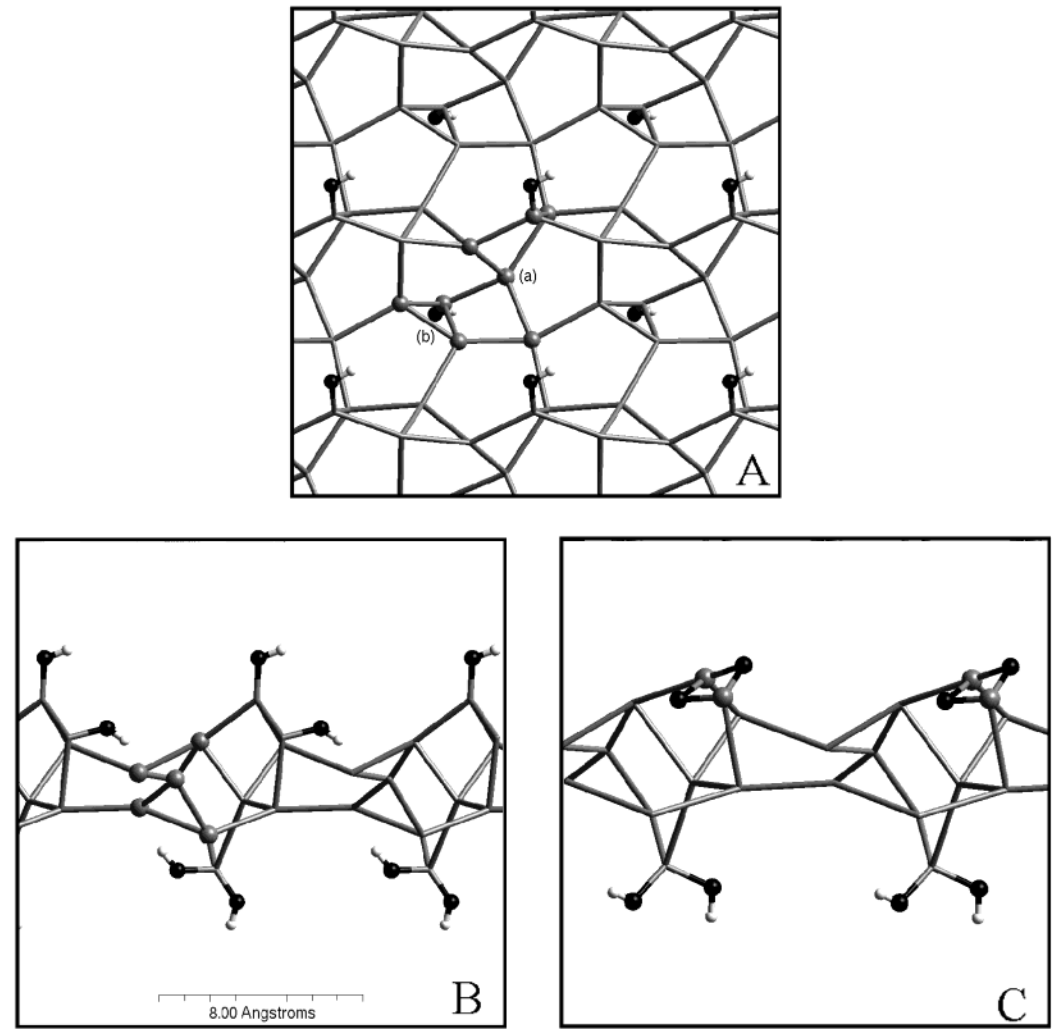

Figure 2. Schematic representation of the three closed shell layers. A: top-view of a snapshot of the S0 structure (top panel); B: side-view of a snapshot of the S1 structure (bottom-left panel); C: side-view of a snapshot of the S2 structure (bottom-right panel). For clarity, only the Si backbone of the three structures has been represented (grey sticks), while the O atoms, with the exception of those of the silanols and of the 2M defect, are not explicitly shown. The atoms forming the silanols and some selected defect centers are highlighted by representing them as spheres. In particular, the labels (a) and (b) in Figure 2A identify, respectively, two adjacent 4-rings and a 3-ring attached to a silanol, whereas in Figure 2B, two vertex-sharing 3-rings are highlighted and in Figure 2C the 2M-ring is shown. Grey spheres: Si; black spheres: O; white spheres: H.

spectra.[5−9,29] Thus, according to both experimental data and simulated excitation spectra the 2M-ring may indeed be present on the surface of MCMs.

Further insight into such issue can be provided by the analysis of the simulated infrared and vibrational spectra of the three closed-shell systems, which were obtained from the dipole moment[43] and velocity autocorrelation functions, respectively. The silica-window region of the calculated IR spectra of S0, S1, and S2 is shown in Figure 4. The frequencies have been corrected for the use of the effective electronic mass in Car-Parrinello simulations by scaling them to the value of the O−H stretching frequencies obtained from a Born−Oppenheimer MD. As expected on the basis of the high concentration of strained Si−O−Si bridges, all of the studied systems show bands inside the silica window. As an example, let us first discuss in detail the S0 spectrum. The two strongest bands, at 852 and 860 cm^{-1}, and the smaller peak at 876 cm^{-1} are due to F_2 modes of the tetrahedron joining the two adjacent 4-rings. The strong band at 866 cm^{-1} is due to an asymmetric Si−O−Si mode of the 3-ring bonded to the silanol, whereas the remaining peaks are modes mainly localized on a second 3-ring. These results indicate that a defect (in this case, the 3-ring) can indeed show

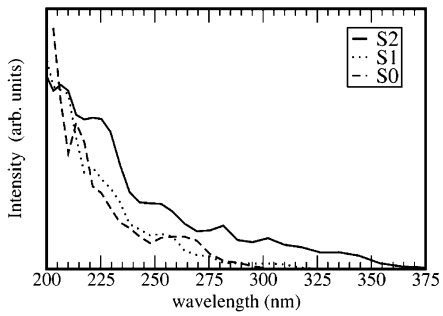

Figure 3. Franck-Condon excitation spectra calculated for the three closed shell systems using for the optical conductivity $\sigma(\omega)$, the formula $\sigma(\omega) = \pi e^2/m^2\omega\ 1/\Omega\sum_{v,c}|\langle\phi_v|\hat{p}|\phi_c\rangle|^2\delta(E_c - E_v - \hbar\omega)$ where e and m are the electronic charge and mass, ω is the frequency, Ω is the cell volume, $\hat{p}$ is the velocity operator, φ_v and φ_c are ground-state wave functions and E_v and E_c ground-state energies of occupied and empty states, respectively. The sum runs on both occupied and empty states. Dashed line refers to S0, dotted line refers to S1 and solid line refers to S2.

different frequencies depending on its local environment. This was also confirmed by the vibrational analysis on the S1 and S2 layers, which contain two vertex-sharing 3-rings. On the

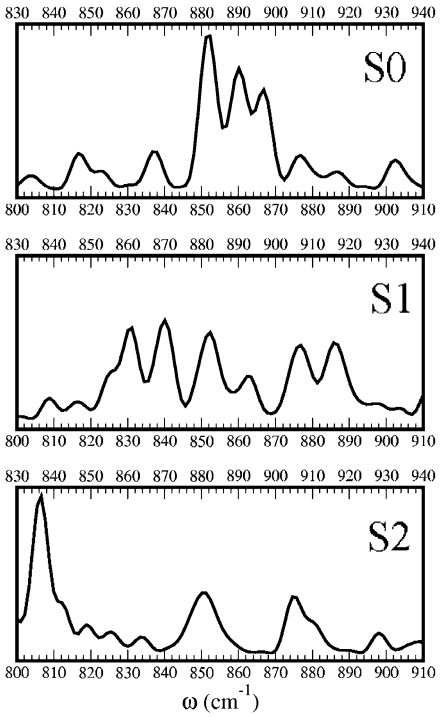

Figure 4. Silica-window region of the IR spectra calculated for S0 (top panel), S1 (middle panel), and S2 (bottom panel). Intensity is in arbitrary units. The calculated wavenumbers are reported on the lower ω-axes. The upper ω axes report shifted wavenumbers obtained by matching the calculated frequency of the Si−OH stretching ($\sim$ 944 cm^{-1}), taken as an "internal reference", to the quoted experimental value for the Si−OH stretching ($\sim$ 975 cm^{-1}).

whole, the calculated frequencies for the above-mentioned defects are not incompatible with the range experimentally found for the SSB bands.

Let us now focus on the S2 spectrum. Analysis of the modes allows us to assign the 806 and 834 cm^{-1} bands to 2M. These frequencies are in the range calculated for this defect on an a-SiO_2 surface (791−841 and 849−856 cm^{-1} depending on the environment).[30] Remarkably, the 806 and 834 cm^{-1} bands are missing in the parent hydrated structure S1. We found also that the presence of 2M perturbs the modes of the neighboring tetrahedra, red-shifting the asymmetric Si−O−Si stretching in passing from S1 to S2. Because of the small size of the simulated system (11 tetrahedral units) the concentration of defects may be significantly higher with respect to experiments; therefore, the perturbing effect of the 2M-ring on the properties of the rest of the slab (and vice versa) is overestimated in our calculations. In this respect, it should be remarked that high-frequency modes, like O−H stretching, are independent of the environment.

The Si−OH stretching mode of isolated silanols in silica materials is characterized by frequencies of about 975 $\pm$ 15 cm^{-1}.[18−20] We may use this mode as an internal reference, as we have found that many defects show frequencies close to the IR region assigned to the reactive SSB. The calculated Si−OH frequency in our layers is 944 $\pm$ 15 cm^{-1}, thus, about 30 cm^{-1} lower than the quoted experimental value. This red shift of 30 cm^{-1} may be considered as the error in the frequency calculation within our computational scheme. The differences between the calculated wavenumbers for the 2M modes (806 and 834 cm^{-1}) and the observed experimental defect bands (890 and 910 cm^{-1}) amount to about 80 cm^{-1}. Such a large difference seems to be in contrast with a straightforward assignment of the IR observed "defect bands" to the 2M structure, and we may consider that 2M might not be the responsible of the SSB IR bands. Such argument is also supported by a combined IR, V−UV, and ESR study on MCM-41 and other a-SiO_2 materials pretreated at high temperatures.[29] The ESR spectra of ref 29 indicate the presence of paramagnetic defects on the dehydroxylated surfaces of these materials, in particular the NBOHC, ≡Si−O•, and the surface E′ center, ≡Si•. In addition, upon exposure to NH_3, both the SSB IR defect bands and the ≡Si−O• and ≡Si• ESR signals disappear, strongly supporting the idea that the highly reactive SSB should be associated to the presence of surface radical centers.[29] Furthermore, according to a Raman/ESR study, the concentration of NBOHC and E′ created by laser irradiation on a-SiO_2 is correlated to the number of strained rings on the surface before irradiation, thus suggesting that ≡Si• and ≡Si−O• radical sites may be generated in pairs by homolytic breaking of Si−O bonds in strained $(Si-O)_n$ rings.[44]

To allow for homolytic bond rupture, we adopted the ROKS formalism because it gives the correct spin state of an open-shell singlet state.[40] This technique provides a formally consistent way to remove the constraint of double orbital occupancy, thus allowing a MD investigation of the effects of the presence of radical centers on the properties of the model layers.

Starting from two different, uncorrelated configurations taken from the closed-shell S2 simulation, two distinct singlet ROKS MD runs were performed. In both cases, after a few fs, we observed the homolytic breaking of a Si−O bond of the 2M-ring, i.e., the most strained ring on the S2 layer. However, two different Si−O bonds are broken in the two simulations. In the first run (simulation a), the outermost Si−O−Si bridge of the 2M defect is broken, leading to a ≡Si−O• dangling bond with the oxygen pointing outward to the vacuum and to a neighboring E′ site (Figure 5A). In contrast, in simulation b, we observed the breaking of the inner Si−O−Si bridge of the 2M defect, not directly exposed to the vacuum (Figure 5B). This event induces the formation of an E′ center and a Si−O• dangling bond that points inside the layer, therefore with the O• atom less accessible to incoming adsorbant molecules. In both cases, the two structures were stable along MD runs of $\sim$10 ps each. This suggests that, at high temperatures, both types of ≡Si−O• dangling bonds may be formed on the surfaces of silica based materials.

The calculated partial vibrational spectra of the Si−O• modes are shown in Figure 6. The frequencies of the Si−O• stretching modes are significantly different in the two cases: the dangling Si−O• pointing outside the surface (run a) has a stretching frequency of 862 cm^{-1}, whereas the Si−O• pointing inward (run b) shows a band at 882 cm^{-1}. These calculated defect bands differ by $\sim$30 cm^{-1} from the experimental SSB IR bands, in line with the frequency shift found for the Si−OH stretching, that is found at 944 cm^{-1} in both radical systems.

These results, together with the findings of ref 29, would strongly suggest the assignment of the two IR defect bands to the stretching modes of two chemically different dangling Si−O• bonds: the ones pointing outside the surface and those pointing inside. Even if these structures emerged from two distinct simulations, it is likely that both kinds of Si−O• sites might be present at the same time on the surface of the real material. It is therefore reasonable to argue that the first set of Si−O• sites, exposed on the surface, should always be easily accessible to incoming reagents. In the case of the inward directed Si−O•, accessibility of bulky molecules is partially limited by the neighboring tetrahedra. This result would provide also a rationalization for experimental data on the reactivity of high-temperature dehydroxylated a-SiO_2 surfaces toward Lewis

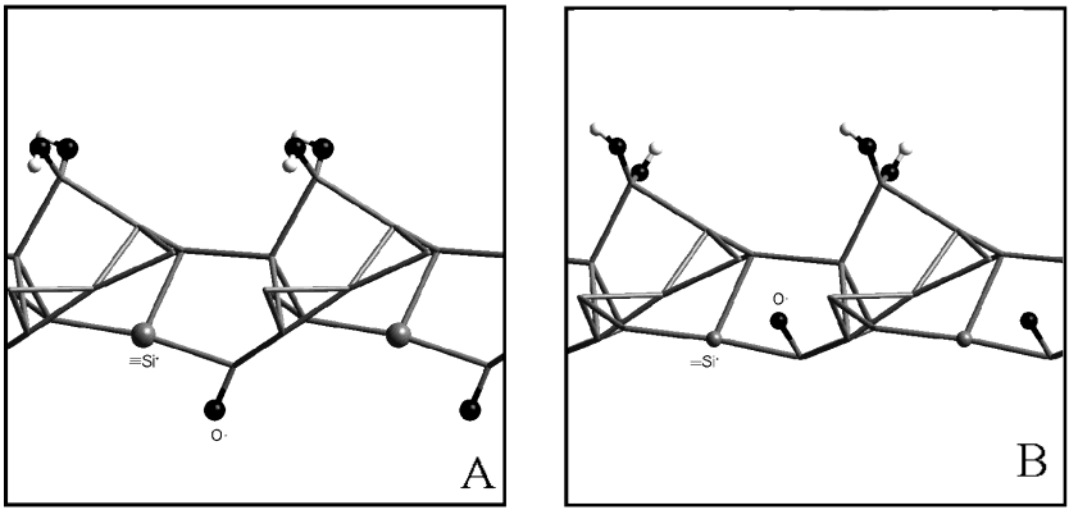

Figure 5. Schematic representation of the layer structures obtained from the two open-shell singlet MD runs. A: a snapshot from simulation a (left panel); B: a snapshot from simulation b (right panel). For clarity, only the Si backbone is represented (by gray sticks). Only the O and H atoms of the silanols and the O and Si atoms of the radical sites (NBOHC and E′ center) are explicitly shown. Grey spheres: Si; black spheres: O; white spheres: H.

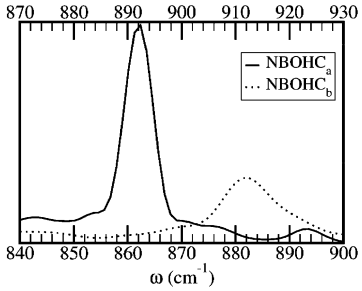

Figure 6. Partial vibrational spectra calculated for the ≡Si−O• modes in simulation a (solid line) and b (dashed line). Intensity is in arbitrary units. The calculated wavenumbers are reported on the lower ω-axes. The upper ω-axes report shifted wavenumbers obtained by matching the calculated frequency of the Si−OH stretching ($\sim$ 944 cm^{-1}), taken as an "internal reference", to the quoted experimental value for the Si−OH stretching ($\sim$ 975 cm^{-1}).

bases.[21−25] It has been reported that, although exposure to small molecules (water, ammonia, methanol, methylamine) leads to the dissociative chemisorption of the adsorbate and to the disappearance of both IR defect bands, upon adsorption of bulky Lewis bases (pyridine, trimethylamine) only the 890 cm^{-1} defect band disappears.[21] These experimental evidences suggested the existence of two kinds of defects whose IR bands and reactivity would be determined from their differing chemical environments.[23] According to our findings, the 890 cm^{-1} band should be that associated to the outward, most accessible, defect sites, on which also large molecules may be easily adsorbed. On the other hand, if the adsorbant molecules are characterized by an high steric hindrance, their accessibility to the innermost defect sites (i.e., the ones we found to be the responsible of the higher frequency defect band) might be precluded. In support to such a hypothesis, kinetic studies of water or ammonia adsorption on high-temperature dehydroxylated a-SiO_2 surfaces found out that in both cases the chemisorption can be rationalized by two processes, both first order with respect to the defect concentration, suggesting that the surface should exhibit two kinds of defects characterized by different kinetic constants.[25]

Conclusions

Different models for the nanothick, inner surfaces of mesoporous silica materials have been studied. On the basis of ab initio simulations and available literature data, the existence of all of the defect structures considered here may be compatible with experimental results. However, other defects currently postulated in silica based materials (e.g., wrong bonds) have not been included in our model. Because of the amorphous nature of the studied system which excludes the existence of a well-defined minimum energy structure, we cannot draw conclusions on the relative stability of the simulated defect structures. On the other hand, comparison of the properties calculated for the model nanothick layers with the available experimental IR, VUV, ESR, and kinetic data on a-silica materials lead us to propose that Si−O• dangling bonds (associated to E′ centers) embedded in two fundamentally different chemical environments could be the most likely "candidates" responsible of the observed IR/ESR defect bands and of the fast dissociative chemisorption of small Lewis bases. We also point out that, by contrast with aluminosilicates, homolytic breaking of bonds upon high temperature pretreatment of silica materials might probably be favored over an heterolytic mechanism because of the absence of ionic species able to stabilize a partially charged transition state. Moreover, even if in our simulation radical species were formed by breaking a 2M-ring, analogous defect structures (i.e., E′ centers and "inner" and "outer" NBOHC), characterized by similar vibrational frequencies, might also arise from the homolytic opening of 3- and 4-cycles. We however should point out that, when spins are localized close to each other, there are many possible mechanisms for broadening and saturating ESR signals,[45] therefore, justifying the absence of paramagnetic signals in some experiments.[21−23] Finally, a realistic picture of the structure of the real MCM surfaces should not exclude the hypothesis that both diamagnetic (i.e., strained rings) structures and paramagnetic defects may exist and that, at the high temperatures adopted in dehydration, such species may be in dynamical equilibrium and could interconvert among each other.

Acknowledgment. We thank INSTM for a computer time grant at CINECA.

References and Notes

(1) Beck, J. S.; Vartuli, J. C.; Roth, W. J.; Leonowicz, M. E.; Kresge, C. T.; Schmitt, K. D.; Chu, C.-T. W.; Olson, D. H.; Sheppard, E. W.; McCullen, S. B.; Higgins, J. B.; Schlenker, J. L. *J. Am. Chem. Soc.* **1992**, *114*, 10834.

(2) Long, Y.; Xu, T.; Sun, Y.; Dong, W. *Langmuir* **1998**, *14*, 6173.
(3) Ying, J. Y.; Mehnert, C. P.; Wong, M. S. *Angew. Chem., Int. Ed. Engl.* **1999**, *38*, 56.
(4) Baerlocher, Ch.; Meier, W. M.; Olson, D. H. *Atlas of Zeolite Framework Types*; Elsevier Science B. V.: Amsterdam, The Netherlands, 2001.
(5) Gimon-Kinsel, M. E.; Groothuis, K.; Balkus, K. J. *Microporous Mesoporous Mater.* **1998**, *20*, 67.
(6) Glinka, Y. D.; Lin, S.-H.; Hwang, L.-P.; Chen, Y. T. *J. Phys. Chem. B* **2000**, *104*, 8652.
(7) Shen, J. L.; Chen, P. N.; Lee, Y. C.; Cheng, C. F. *Solid State Commun.* **2002**, *122*, 65.
(8) Glinka, Y. D.; Zyubin, A. S.; Mebel, A. M.; Lin, S.-H.; Hwang, L.-P.; Chen, Y. T. *Chem. Phys. Lett.* **2002**, *358*, 180.
(9) Zyubin, A. S.; Glinka, Y. D.; Mebel, A. M.; Lin, S.-H.; Hwang, L.-P.; Chen, Y. T. *J. Chem. Phys.* **2002**, *116*, 281.
(10) Skuja, L. *J. Non.-Cryst. Solids* **1994**, *179*, 51.
(11) Skuja, L. *J. Non.-Cryst. Solids* **1998**, *239*, 16.
(12) Pacchioni, G.; Ierano', G. *Phys. Rev. B* **1998**, *57*, 818.
(13) Miller, A. J.; Leisure, R. G.; Austin, Wm. R. *J. Appl. Phys.* **1999**, *86*, 2042.
(14) Glinka, Y. D.; Lin, S.-H.; Chen, Y. T. *Phys. Rev. B* **2000**, *62*, 4733.
(15) Hosono, H.; Kaijhara, K.; Suzuki, T.; Ikuta, Y.; Skuja, L.; Hirano, M. *Solid State Commun.* **2002**, *122*, 117.
(16) Zecchina, A.; Bordiga, S.; Spoto, G.; Marchese, L.; Petrini, G.; Leofanti, L.; Padovan, M. *J. Phys. Chem.* **1992**, *96*, 4991.
(17) Creighton, J. A.; Deckman, H. W.; Newsam, J. M. *J. Phys. Chem.* **1994**, *98*, 448.
(18) Zhao, X. S.; Lu, G. Q.; Hu, X. *Microporous Mesoporous Mater.* **2000**, *41*, 37.
(19) Eimer, G. A.; Pierella, L. B.; Monti, G. A.; Anunziata, O. A. *Catal. Lett.* **2002**, *78*, 65.
(20) Zecchina, A.; Bordiga, S.; Spoto, G.; Marchese, L.; Petrini, G.; Leofanti, L.; Padovan, M. *J. Phys. Chem.* **1992**, *96*, 4985.
(21) Morrow, B. A.; Cody, I. A. *J. Phys. Chem.* **1976**, *80*, 1995.
(22) Morrow, B. A.; Cody, I. A. *J. Phys. Chem.* **1976**, *80*, 1998.
(23) Morrow, B. A.; Cody, I. A.; Lee, L. S. M. *J. Phys. Chem.* **1976**, *80*, 2761.
(24) Bunker, B. C.; Haaland, D. M.; Ward, K. T.; Michalske, T. A.; Smith, W. L.; Binkley, J. S.; Melius, C. F.; Balfe, C. A. *Surf. Sci.* **1989**, *210*, 406.
(25) Bunker, B. C.; Haaland, D. M.; Michalske, T. A.; Smith, W. L. *Surf. Sci.* **1989**, *222*, 95.
(26) Dubois, L. H.; Zegarski, B. R. *J. Am. Chem. Soc.* **1993**, *115*, 1190.
(27) Grabbe, A.; Michalske, T. A.; Smith, W. L. *J. Phys. Chem.* **1995**, *99*, 4648.
(28) Gianotti, E.; Dellarocca, V.; Marchese, L.; Martra, G.; Coluccia, S.; Maschmeyer, T. *Phys. Chem. Chem. Phys.* **2002**, *4*, 6109.
(29) Inaki, Y.; Hisao, Y.; Yoshida, T.; Hattori, T. *J. Phys. Chem.* **2002**, *106*, 9098.
(30) Ceresoli, D.; Bernasconi, M.; Iarlori, S.; Parrinello, M.; Tosatti, E. *Phys. Rev. Lett.* **2000**, *84*, 3787.
(31) Galeener, F. L.; Barrio, R. A.; Martinez, E.; Elliot, R. J. *Phys. Rev. Lett.* **1984**, *53*, 2429.
(32) Car, R.; Parrinello, M. *Phys. Rev. Lett.* **1985**, *55*, 2471.
(33) Marchese, L.; Gianotti, E.; Dellarocca, V.; Maschmeyer, T.; Rey, F.; Coluccia, S.; Thomas, J. M. *Phys. Chem. Chem. Phys* **1999**, *1*, 585.
(34) *CPMD 3.5*, written by J. Hutter et al., MPI für Festkörperforschung and IBM Research Laboratory.
(35) Becke, A. D. *Phys. Rev. A* **1988**, *38*, 3098.
(36) Perdew, J. P. *Phys. Rev. B* **1986**, *33*, 8822.
(37) Kleinman, L.; Bylander, D. *Phys. Rev. Lett.* **1982**, *48*, 1425.
(38) Troullier, N.; Martins, J. *Phys. Rev. B* **1991**, *43*, 1993.
(39) Nose, S. *J. Chem. Phys.* **1984**, *81*, 511.
(40) Frank, I.; Hutter, J.; Mark, D.; Parrinello, M. *J. Chem. Phys.* **1998**, *108*, 4060.
(41) Müller, U. *Inorganic Structural Chemistry*; J. Wiley & Sons Ltd.: Chichester, U.K., 1993.
(42) Fois, E.; Gamba, A.; Tabacchi, G. *J. Phys. Chem. B* **1998**, *102*, 3974.
(43) Resta, R. *Phys. Rev. Lett.* **1998**, *80*, 1800.
(44) Hosono, H.; Ikuta, Y.; Kinoshita, T.; Kajihara, K.; Hirano, M. *Phys. Rev. Lett.* **2001**, *87*, 175501.
(45) Pake, G. E.; Tuttle, T. R. *Phys. Rev. Lett.* **1959**, *3*, 423.